chapter 6

Interaction of Radiation with Matter

The two most important general types of radiation emitted during radioactive decay are *charged particles*, such as α particles and β particles, and *electromagnetic radiation* (photons), such as γ rays and x rays. These radiations transfer their energy to matter as they pass through it. The principle mechanisms for energy transfer are ionization and excitation of atoms and molecules. Most of this energy ultimately is degraded into heat (atomic and molecular vibrations); however, the ionization effect has other important consequences. For this reason, the radiations emitted during radioactive decay often are called *ionizing radiations*. The processes by which ionizing radiations transfer their energy to matter are fundamental to the detection of radiation, discussed in Chapter 7. As well, they are important for radiation dosimetry, discussed in Chapter 22. In this chapter, we discuss those processes in some detail. Because the mechanisms differ, they are discussed separately for particulate versus electromagnetic radiation.

A. INTERACTIONS OF CHARGED PARTICLES WITH MATTER

1. Charged-Particle Interaction Mechanisms

High-energy charged particles, such as α particles or β particles, lose energy and slow down as they pass through matter, as a result of collisions with atoms and molecules. High-energy electrons, which also are charged particles, are a byproduct of these collisions. In addition, high-energy electrons are generated when γ rays and x rays interact with matter, and they are emitted in internal conversion (see Chapter 3, Section E) and in the Auger effect (see Chapter 2, Section C.3).

For these reasons, this section emphasizes the interactions of electrons with matter. Except for differences in sign, the forces experienced by positive and negative electrons (e.g., β^+ and β^- particles) are identical. There are minor differences between the ionizing interactions of these two types of particles, but they are not of importance to nuclear medicine and are not discussed here. In this chapter, the term *electrons* is meant to include both the positive and negative types. The annihilation effect, which occurs when a positive electron (positron) has lost all of its kinetic energy and stopped, is discussed in Chapter 3, Section G.

The "collisions" that occur between a charged particle and atoms or molecules involve electrical forces of attraction or repulsion rather than actual mechanical contact. For example, a charged particle passing near an atom exerts electrical forces on the orbital electrons of that atom. In a close encounter, the strength of the forces may be sufficient to cause an orbital electron to be separated from the atom, thus causing ionization (Fig. 6-1A). An ionization interaction looks like a collision between the charged particle and an orbital electron. The charged particle loses energy in the collision. Part of this energy is used to overcome the binding energy of the electron to the atom, and the remainder is given to the ejected *secondary electron* as kinetic energy. Ionization involving an inner-shell electron eventually leads to the emission of characteristic x rays or Auger electrons; however, these effects generally are very small, because most ionization interactions involve outer-shell electrons. The ejected electron may be sufficiently energetic to cause *secondary ionizations* on its own. Such an electron is called a *delta* (δ) *ray*.

A less-close encounter between a charged particle and an atom may result in an orbital electron being raised to an *excited state,* thus

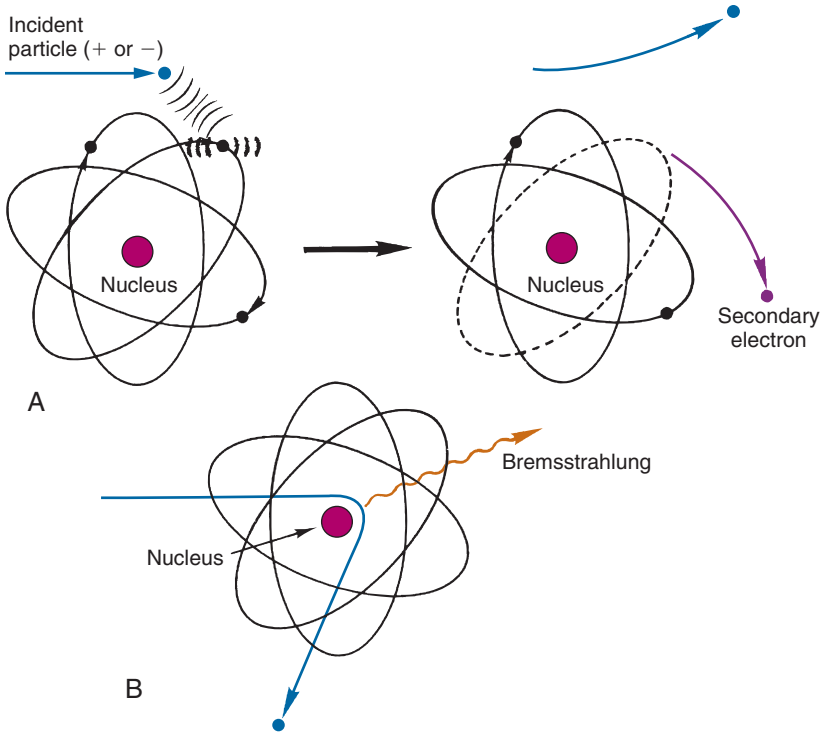

FIGURE 6-1 Interactions of charged particles with atoms. *A,* Interaction with an orbital electron resulting in ionization. Less-close encounters may result in atomic excitation without ionization. *B,* Interaction with a nucleus, resulting in bremsstrahlung production. [*Repulsion by orbital electron (A) and attraction toward nucleus (B) indicates incident particles are negatively charged in the examples shown.*]

causing atomic or molecular *excitation*. These interactions generally result in smaller energy losses than occur in ionization events. The energy transferred to an atom in an excitation interaction is dissipated in molecular vibrations, atomic emission of infrared, visible, ultraviolet radiation, and so forth.

A third type of interaction occurs when the charged particle actually penetrates the orbital electron cloud of an atom and interacts with its nucleus. For a heavy charged particle of sufficiently high energy, such as an α particle or a proton, this may result in nuclear reactions of the types used for the production of radionuclides (see Chapter 5); however, for both heavy charged particles and electrons, a more likely result is that that particle will simply be deflected by the strong electrical forces exerted on it by the nucleus (Fig. 6-1B). The particle is rapidly decelerated and loses energy in the "collision." The energy appears as a photon of electromagnetic radiation, called *bremsstrahlung* (German for "braking radiation").

The energy of bremsstrahlung photons can range anywhere from nearly zero (events in which the particle is only slightly deflected) up to a maximum equal to the full energy of the incident particle (events in which the particle is virtually stopped in the collision). Figure 6-2 shows the energy spectrum for bremsstrahlung photons generated in aluminum by particles from a ^{90}Sr-^{90}Y source mixture (E_β^{max} = 2.27 MeV) and illustrates that most of the photons are in the lower energy range.

2. Collisional Versus Radiation Losses

Energy losses incurred by a charged particle in ionization and excitation events are called *collisional losses,* whereas those incurred in nuclear encounters, resulting in bremsstrahlung production, are called *radiation losses.* In the nuclear medicine energy range, collisional losses are by far the dominating factor (See Fig. 6-5). Radiation losses increase with increasing particle energy and with increasing atomic number of the absorbing medium. An approximation for percentage radiation losses for β particles having maximum energy E_β^{max} (MeV) is

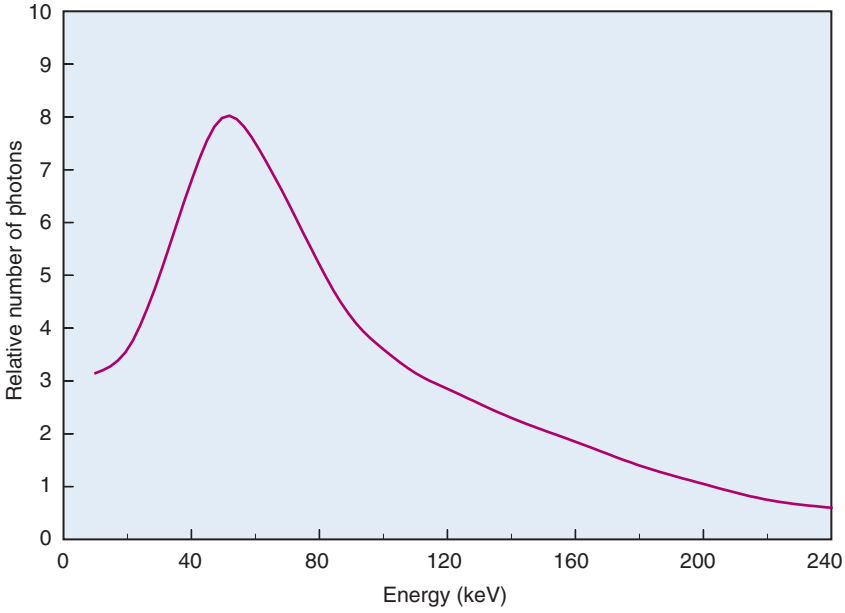

FIGURE 6-2 Bremsstrahlung spectrum for β particles emitted by ^{90}Sr + ^{90}Y (E_β^{max} = 2.27 MeV) mixture in aluminum. (*Adapted from Mladjenovic M:* Radioisotope and Radiation Physics. *New York, 1973, Academic Press, p 121.*)

$$\text{percentage radiation losses} \approx (ZE_\beta^{max}/3000) \times 100\% \quad (6\text{-}1)$$

where Z is the atomic number of the absorber. This approximation is accurate to within approximately 30%. For a mixture of elements, an "effective" atomic number for bremsstrahlung production should be used

$$Z_{eff} = \sum_i f_i Z_i^2 \Big/ \sum f_i Z_i \quad (6\text{-}2)$$

where $f_1, f_2, \ldots$ are the fractions by weight of the elements $Z_1, Z_2, \ldots$ in the mixture.

EXAMPLE 6-1

Calculate the percentage of radiation losses for ^{32}P β particles in water and in lead.

Answer

E_β^{max} = 1.7 MeV for ^{32}P. Water comprises $^{2}/_{18}$ parts hydrogen (Z = 1, AW ≈ 1) and $^{16}/_{18}$ parts oxygen (Z = 8, AW ≈ 16); thus its effective atomic number for bremsstrahlung production is (Equation 6-2)

$$Z_{eff} = \frac{[(1/9)(1)^2(8/9)(8)^2]}{[(1/9)(1)+(8/9)(8)]} = 7.9$$

The percentage of radiation losses in water are therefore (Equation 6-1)

$$(7.9 \times 1.7/3000) \times 100\% \approx 0.4\%$$

and in lead (Z = 82) they are

$$(82 \times 1.7/3000) \times 100\% \approx 4.6\%$$

The remaining 99.6% and 95.4%, respectively, are dissipated as collisional losses.

Example 6-1 demonstrates that high-energy electrons in the nuclear medicine energy range dissipate most of their energy in collisional losses. Bremsstrahlung production accounts for only a small fraction of their energy. Nevertheless, bremsstrahlung can be important in some situations, such as the shielding of relatively large quantities of an energetic β-particle emitter (e.g., hundreds of MBq of ^{32}P). The β particles themselves are easily stopped by only a few millimeters of plastic, glass, or lead (see Section B.2); however, the bremsstrahlung photons they generate are much more penetrating and may require additional shielding around the primary β-particle shielding. It is helpful in such situations to use a low-Z material, such as plastic, for the primary β-particle shielding, and then to surround this with a higher-Z material, such as lead, for bremsstrahlung shielding (Fig. 6-3). This arrangement minimizes bremsstrahlung production by the β particles in the shielding material.

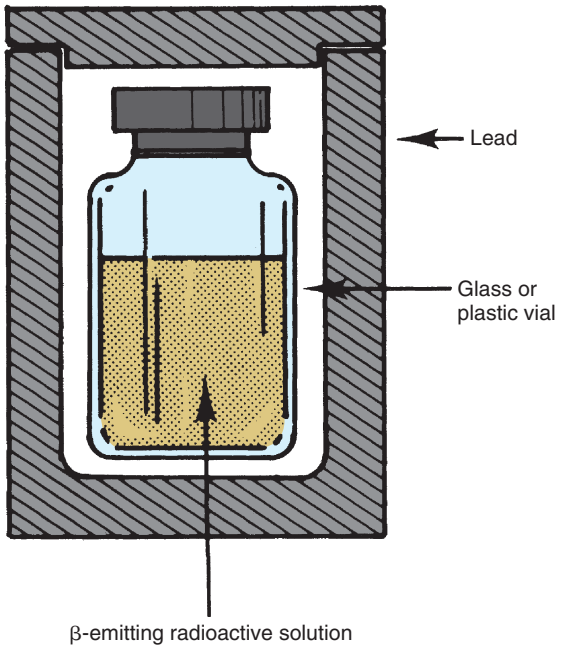

FIGURE 6-3 Preferred arrangement for shielding energetic β-emitting radioactive solution. Glass or plastic walls of a vial stop the β particles with minimum bremsstrahlung production, and a lead container absorbs the few bremsstrahlung photons produced.

Bremsstrahlung production and radiation losses for α particles and other heavy charged particles are very small because the amount of bremsstrahlung production is inversely proportional to the mass of the incident charged particle. Alpha particles and protons are thousands of times heavier than electrons and therefore dissipate only a few hundredths of 1% or less of their energy as radiation losses. These particles, even at energies up to 100 MeV, dissipate nearly all of their energy as collisional losses.

3. Charged-Particle Tracks

A charged particle passing through matter leaves a track of secondary electrons and ionized atoms in its path. In soft tissue and materials of similar density, the tracks are typically approximately 100 μm wide, with occasionally longer side tracks generated by energetic δ rays. The tracks are studied in nuclear physics using film emulsions, cloud chambers,* and other devices.

When a heavy particle, such as an α particle, collides with an orbital electron, its direction is virtually unchanged and it loses only a small fraction of its energy (rather like a bowling ball colliding with a small lead shot). The maximum fractional energy loss by a heavy particle of mass M colliding with a light particle of mass m is approximately $4\,m/M$. For an α particle colliding with an electron, this amounts to only approximately 0.05% [$4 \times (1/1840)/4 \approx (1/2000)$]. Heavy particles also undergo relatively few bremsstrahlung-producing collisions with nuclei. As a result, their tracks tend to be straight lines, and they experience an almost continuous slowing down in which they lose small amounts of energy in a large number of individual collisions.

By contrast, electrons can undergo large-angle deflections in collisions with orbital electrons and can lose a large fraction of their energy in these collisions. These events are more like collisions between billiard balls of equal mass. Electrons also undergo occasional collisions with nuclei in which they are deflected through large angles and bremsstrahlung photons are emitted. For these reasons, electron tracks are tortuous, and their exact shape and length are unpredictable.

An additional difference between electrons and heavy particles is that for a given amount of kinetic energy, an electron travels at a much faster speed. For example, a 4-MeV α particle travels at approximately 10% of the speed of light, whereas a 1-MeV electron travels at 90% of the speed of light. As a result, an electron spends a much briefer time in the vicinity of an atom than does an α particle of similar energy and is therefore less likely to interact with the atom. Also, an electron carries only one unit of electrical charge, versus two for α particles, and thus exerts weaker forces on orbital electrons. For these reasons, electrons experience less frequent interactions and lose their energy more slowly than α particles; they are much less densely ionizing, and they travel farther before they are stopped than α particles or other heavy charged particles of similar energy.

To illustrate these differences, Figure 6-4 shows (in greatly enlarged detail) some

*A cloud chamber consists of a cylinder with a piston at one end and viewing windows at the other end and around the sides. The cylinder contains a water-alcohol vapor mixture under pressure. When the piston is rapidly withdrawn to suddenly decrease the pressure and temperature of the vapor, droplets of condensed liquid are formed around ionized nuclei. Ionization tracks existing in the chamber at the time thus can be observed and photographed through the viewing windows.

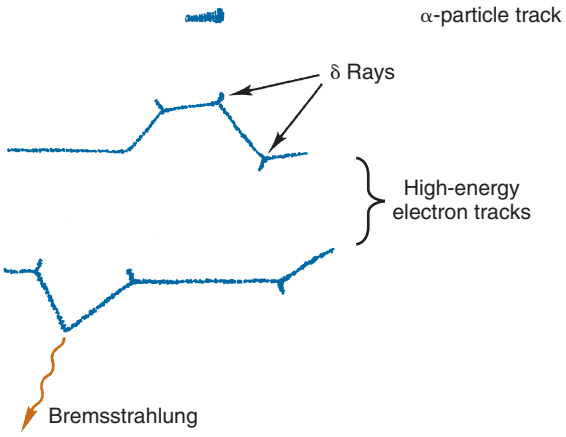

FIGURE 6-4 Representation of α particle and electron tracks in an absorber. Alpha particles leave short, straight, densely ionized tracks, whereas electron paths are tortuous and much longer; δ rays are energetic secondary electrons.

possible tracks for β particles and for α particles in water. The actual track lengths are on the order of microns for α particles and fractions of a centimeter for β particles. This is discussed further in Section B.

4. Deposition of Energy Along a Charged-Particle Track

The rate at which a charged particle loses energy determines the distance it will travel and the density of ionization along its track. Energy loss rates and ionization densities depend on the type of particle and its energy and on the composition and density of the absorbing medium. Density affects energy loss rates because it determines the density of atoms along the particle path. In the nuclear medicine energy range (≲10 MeV), energy loss rates for charged particles increase linearly with the density of the absorbing medium. (At higher energies, density effects are more complicated, as discussed in the sources cited in the references and bibliography at the end of this chapter.)

Figure 6-5 shows collisional and radiation energy loss rates for electrons in the energy range of 0.01-10 MeV in water and in lead. Energy loss rates $\Delta E/\Delta x$ are expressed in MeV/g • cm^{-2} to normalize for density effects

$$\Delta E/\Delta x\ (\text{MeV/g} \cdot \text{cm}^{-2}) = \frac{\Delta E/\Delta x\ (\text{MeV/cm})}{\rho\ (\text{g/cm}^3)} \tag{6-3}$$

Thus for a given density ρ the energy loss rate in MeV/cm is given by

$$\Delta E/\Delta x\ (\text{MeV/cm}) = [\Delta E/\Delta x\ (\text{MeV/g} \cdot \text{cm}^{-2})] \times \rho\ (\text{g/cm}^3) \tag{6-4}$$

Collisional loss rates $\Delta E/\Delta x_{\text{coll}}$ decrease with increasing electron energy, reflecting the velocity effect mentioned in Section A.3. Also,

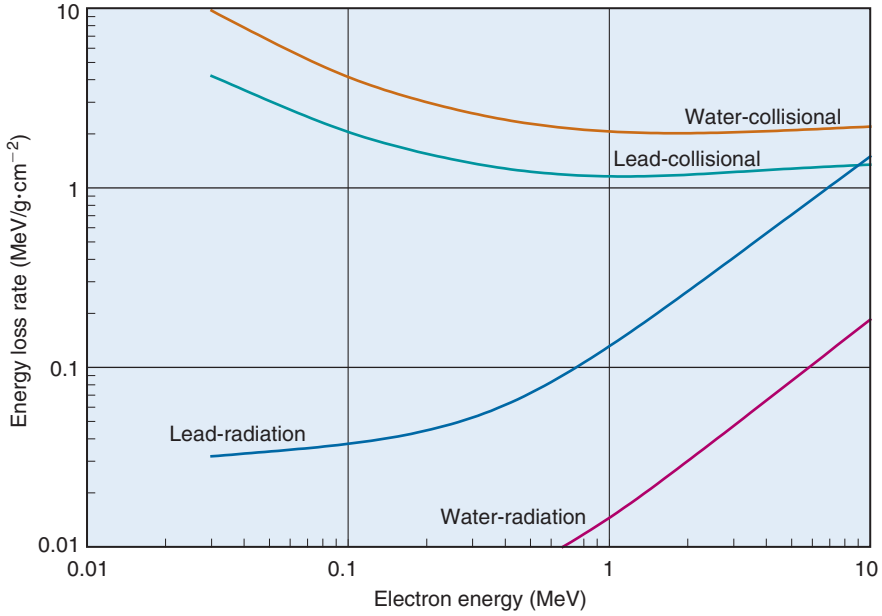

FIGURE 6-5 Collisional (ionization, excitation) and radiation (bremsstrahlung) energy losses versus electron energy in lead and in water. (*Adapted from Johns HE, Cunningham JR:* The Physics of Radiology, *3rd ed. Springfield, IL, 1971, Charles C Thomas, p 47.*)

$\Delta E/\Delta x_{coll}$ decreases with increasing atomic number of the absorbing medium because in atoms of higher atomic number, inner-shell electrons are "screened" from the incident electron by layers of outer-shell electrons, making interactions with inner-shell electrons less likely in these atoms. Gram for gram, lighter elements are better absorbers of electron energy than are heavier elements.

Radiation loss rates $\Delta E/\Delta x_{rad}$ increase with increasing electron energy and increasing atomic number of the absorber. This is discussed in Section A.2.

The total energy loss rate of a charged particle, $\Delta E/\Delta x_{total}$, expressed in MeV/cm, is also called the *linear stopping power* (S_l). A closely related parameter is the *linear energy transfer* (LET), L, which refers to energy lost that is deposited "locally" along the track. L differs from S_l in that it does not include radiation losses. These result in the production of bremsstrahlung photons, which may deposit their energy at some distance from the particle track. For both electrons and α particles in the nuclear medicine energy range, however, radiation losses are small, and the two quantities S_l and L are practically identical.

The average value of the linear energy transfer measured along a charged-particle track, $\overline{L}$, is an important parameter in health physics (see Chapter 23, Section A.1.). $\overline{L}$ usually is expressed in units of keV/μm. For electrons in the energy range of 10 keV to 10 MeV traveling through soft tissue, $\overline{L}$ has values in the range of 0.2-2 keV/μm. Lower-energy electrons, for example, β particles emitted by ^{3}H ($\overline{E}_\beta = 5.6$ keV), have somewhat higher values of $\overline{L}$. Alpha particles have values of $\overline{L} \approx 100$ keV/μm.

Specific ionization (SI) refers to the total number of ion pairs produced by both primary and secondary ionization events per unit of track length along a charged particle track. The ratio of linear energy transfer divided by specific ionization is W, the *average energy expended per ionization event:*

$$W = L/\mathrm{SI} \qquad (6\text{-}5)$$

This quantity has been measured and found to have a relatively narrow range of values in a variety of gases (25-45 eV per ion pair or, equivalently, per ionization) independent of the type or energy of the incident particle. The value for air is 33.7 eV per ion pair. W is not the same as the *ionization potential* (I), which is the average energy *required* to cause an ionization in a material (averaged over all the electron shells). Ionization potentials for gases are in the range 10-15 eV. The difference between W and I is energy dissipated by a charged particle in nonionizing excitation events. Apparently, more than half of the energy of a charged particle is expended in this way. Similar ratios between W and I are found in semiconductor solids, except that in these materials the values of W and I are both approximately a factor of 10 smaller than for gases (see Table 7-1).

Because W does not change appreciably with particle type or energy, specific ionization is proportional to linear energy transfer L along a charged particle track. Figure 6-6 shows specific ionization in air for electrons as a function of their energy. The curve indicates that specific ionization increases with decreasing energy down to an energy of approximately 100 eV. This behavior reflects the fact that energy loss rates and L increase as the electron slows down. Below approximately 100 eV, the electron energy is inadequate to cause ionizations efficiently, and specific ionization decreases rapidly to zero.

Specific ionization values for α particles are typically 100 times greater than for electrons of the same energy because of their greater charge and much lower velocities. This leads to greater rates of energy loss, as discussed in previously in Section A.3.

The fact that specific ionization increases as a particle slows down leads to a marked increase in ionization density near the end of its track. This effect is especially pronounced for heavy particles. Figure 6-7 shows a graph of ionization density versus distance traveled for α particles in air. The peak near the end of the α-particle range is called the *Bragg ionization peak.*[*] A similar increase in ionization density is seen at the end of an electron track; however, the peak occurs when the electron energy has been reduced to less than approximately 1 keV, and it accounts for only a small fraction of its total energy.

5. The Cerenkov Effect

An additional charged-particle interaction deserving brief mention is the *Cerenkov* (pronounced cher-en′-kof) *effect.* This effect occurs when a charged particle travels in a medium at a speed greater than the speed of light in that medium. The restriction that a particle

[*]Advantage is taken of this peak in radiation therapy using high-energy protons. The energy of protons is adjusted so that the Bragg peak occurs within the tumor or other treated tissue.

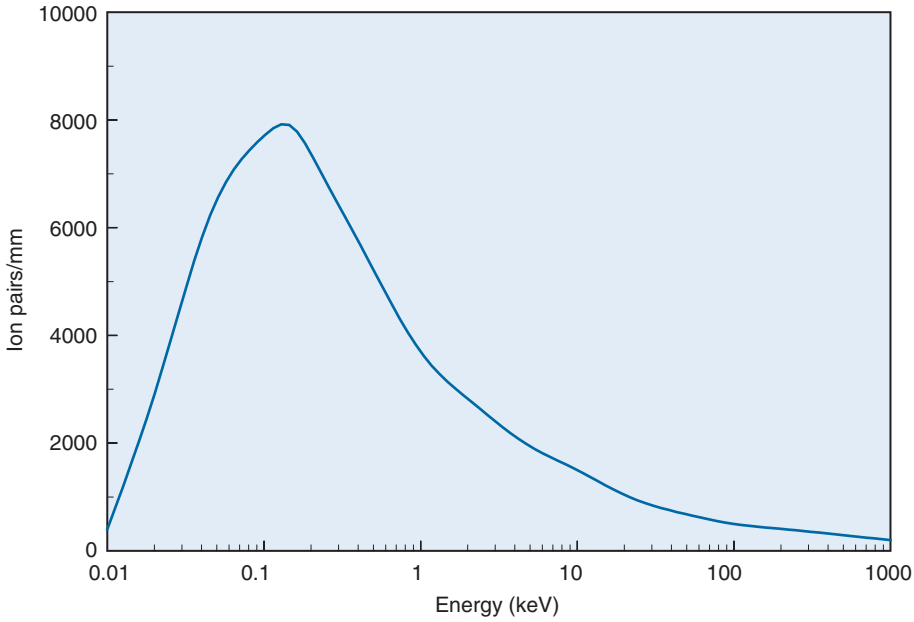

FIGURE 6-6 Specific ionization for electrons versus energy in water. (*Adapted from Mladjenovic M:* Radioisotope and Radiation Physics. *New York, 1973, Academic Press, p 145.*)

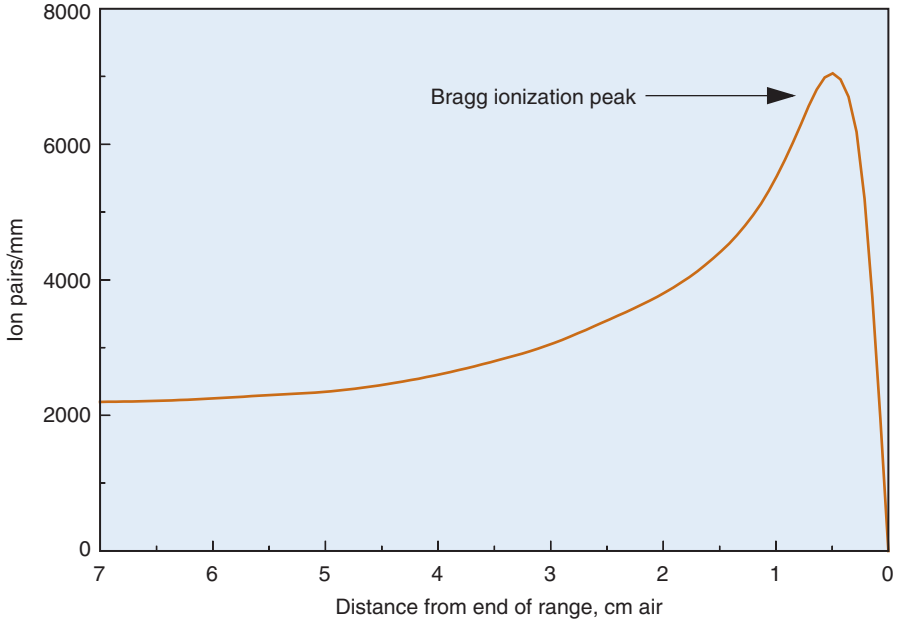

FIGURE 6-7 Specific ionization versus distance traveled for α particles in air. (*Adapted from Mladjenovic M:* Radioisotope and Radiation Physics. *New York, 1973, Academic Press, p 111.*)

cannot travel faster than the speed of light applies to the speed of light in a vacuum ($c \approx 3 \times 10^8$ m/sec); however, a 1-MeV β particle emitted in water travels with a velocity of $v \approx 0.8\,c$, whereas the speed of light in water (refractive index $n = 1.33$) is $c' = c/n \approx 0.75\,c$. Under these conditions, the particle creates an electromagnetic "shock wave" in much the same way that an airplane traveling faster than the speed of sound creates an

acoustic shock wave. The electromagnetic shock wave appears as a burst of visible radiation, typically bluish in color, called *Cerenkov radiation*. The Cerenkov effect can occur for electrons with energies of a few hundred keV; however, for heavy particles such as α particles and protons, energies of several thousands of MeV are required to meet the velocity requirements.

The Cerenkov effect accounts for a very small fraction (<1%) of electron energies in the nuclear medicine energy range, but it is detectable in water solutions containing an energetic β-particle emitter (e.g., ^{32}P) using a liquid scintillation-counting apparatus. The Cerenkov effect also is responsible for the bluish glow that is seen in the water around the core of an operating nuclear reactor.

B. CHARGED-PARTICLE RANGES

1. Alpha Particles

An α particle loses energy in a more or less continuous slowing-down process as it travels through matter. The particle is deflected only slightly in its collisions with atoms and orbital electrons. As a result, the distance traveled, or *range*, of an α particle depends only on its initial energy and on its average energy loss rate in the medium. For α particles of the same energy, the range is quite consistent from one particle to the next. A transmission curve, showing percent transmission for α particles versus thickness of absorber, remains essentially flat at 100% until the maximum range is reached; then it falls rapidly to zero (Fig. 6-8). The *mean range* is defined as the thickness resulting in 50% transmission. There is only a small amount of range fluctuation, or *range straggling*, about the mean value. Typically, range straggling amounts to only approximately 1% of the mean range.

For α particles emitted in radioactive decay (E = 4-8 MeV), an approximation for the mean range in air is

$$R(\text{cm}) \approx 0.325\, E^{3/2}(\text{MeV}) \qquad (6\text{-}6)$$

EXAMPLE 6-2

Calculate the mean range in air of α particles emitted by ^{241}Am (E_α = 5.49 MeV).

Answer

$$R(\text{cm}) = 0.325 \times (5.49)^{3/2}$$
$$= 0.325 \times (\sqrt{5.49})^3$$
$$\approx 4.2 \text{ cm}$$

Example 6-2 illustrates that α particles have very short ranges. They produce densely ionized tracks over this short range.

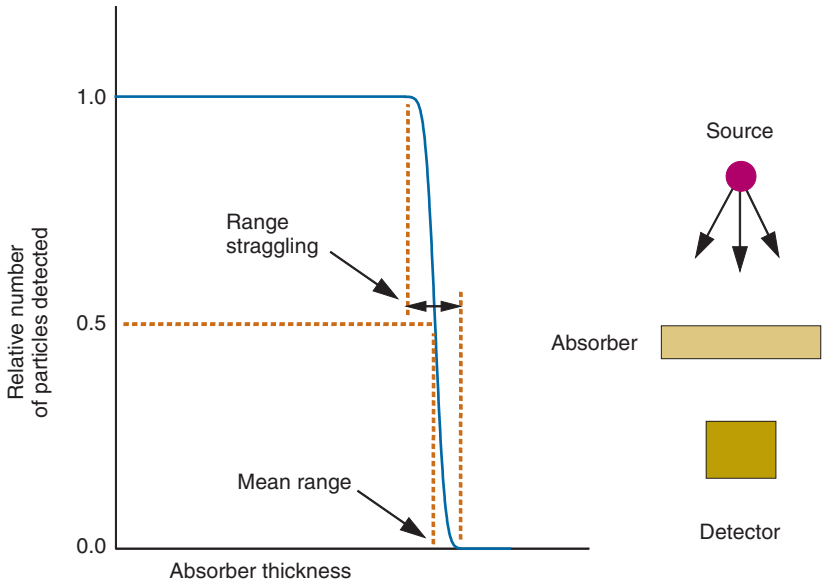

FIGURE 6-8 Relative number of particles detected versus absorber thickness in a transmission experiment with α particles. Range straggling is exaggerated for purposes of illustration.

EXAMPLE 6-3

Estimate the average value of specific ionization in air for α particles emitted by ^{241}Am.

Answer

W = 33.7 eV/ion pair in air. Therefore the number N of ionizations caused by an α particle of energy 5.49 MeV is

$$N = 5.49 \times 10^6 \text{ eV}/33.7 \text{ eV/ion pair}$$
$$\approx 1.63 \times 10^5 \text{ ion pairs}$$

Over a distance of travel of 4.2 cm, the average specific ionization is therefore

$$\overline{\text{SI}} \approx 1.63 \times 10^5 \text{ ion pairs}/4.2 \text{ cm}$$
$$\approx 3.9 \times 10^4 \text{ ion pairs/cm}$$
$$\approx 3.9 \times 10^3 \text{ ion pairs/mm}$$

Compare the result in Example 6-3 with the values shown in Figures 6-6 and 6-7. Only near the very end of their ranges (E & 1 keV) do electrons have specific ionizations comparable to the *average* values for α particles.

Alpha particle ranges in materials other than air can be estimated using the equation

$$R_x = R_{air}\left(\frac{\rho_{air}\sqrt{A_x}}{\rho_x\sqrt{A_{air}}}\right) \qquad (6\text{-}7)$$

where R_{air} is the range of the α particle in air, ρ_{air} (=0.001293 g/cm^3) and A_{air} (≈14) are the density and (average) mass number of air, and ρ_x and A_x are the same quantities for the material of interest. This estimation is accurate to within approximately 15%.

EXAMPLE 6-4

What is the approximate mean range of α particles emitted by ^{241}Am in soft tissue? Assume that ρ_{tissue} = 1 g/cm^3.

Answer

The elemental compositions of air and soft tissue are similar; thus $A_{air} \approx A_x$ may be assumed. From Example 6-2, $R_{air} \approx 4.2$ cm. Therefore the approximate range in soft tissue is

$$R_{tissue} \approx 4.2 \text{ cm} \times (0.001293 \text{ g/cm}^3)/(1 \text{ g/cm}^3)$$
$$\approx 0.0054 \text{ cm}$$
$$\approx 54 \text{ μm}$$

Examples 6-2 and 6-4 illustrate that α particles have very short ranges in air as well as in soft tissue and other solid materials. The very short ranges of α particles mean that they constitute an almost negligible hazard as an external radiation source. Only a few centimeters of air, a sheet of paper, or a rubber glove provides adequate shielding protection. Even those particles that do reach the skin deliver a radiation dose only to the most superficial layers of skin. Alpha particle emitters become a radiation hazard only when ingested; then, because of their densely ionizing nature, they become very potent radiation hazards. (See Chapter 22, Section A and Chapter 23, Section A.).

2. Beta Particles and Electrons

Alpha particles travel in straight lines. Thus their path lengths (total length of path traveled) and ranges (thickness of material required to stop them) are essentially equal. This does not apply to electrons, which can undergo sharp deflections along their path or be stopped completely in a single interaction. Electron ranges are quite variable from one electron to the next, even for electrons of exactly the same energy in the same absorbing material. Path lengths are an important parameter for calculating linear energy transfer. Ranges are important for radiation dosimetry (Chapter 22) and radiation protection (Chapter 23), and for determining the limiting spatial resolution of positron imaging devices (Chapter 18). For this reason, the following discussions focus on electron ranges.

A transmission experiment with β particles results in a curve of the type illustrated in Figure 6-9. Transmission begins to decrease immediately when absorber is added because even thin absorbers can remove a few electrons by the processes mentioned earlier. When the transmission curve is plotted on a semilogarithmic scale, it follows at first a more or less straight-line decline until it gradually merges with a long, relatively flat tail. The tail of the curve does not reflect β-particle transmission but rather represents the detection of relatively penetrating bremsstrahlung photons generated by the β particles in the absorber and possibly in the source and source holder. Extraneous instrument and radiation background also may contribute to the tail of the curve.

The thickness of absorber corresponding to the intersection between the extrapolation of the linearly descending portion and the tail of

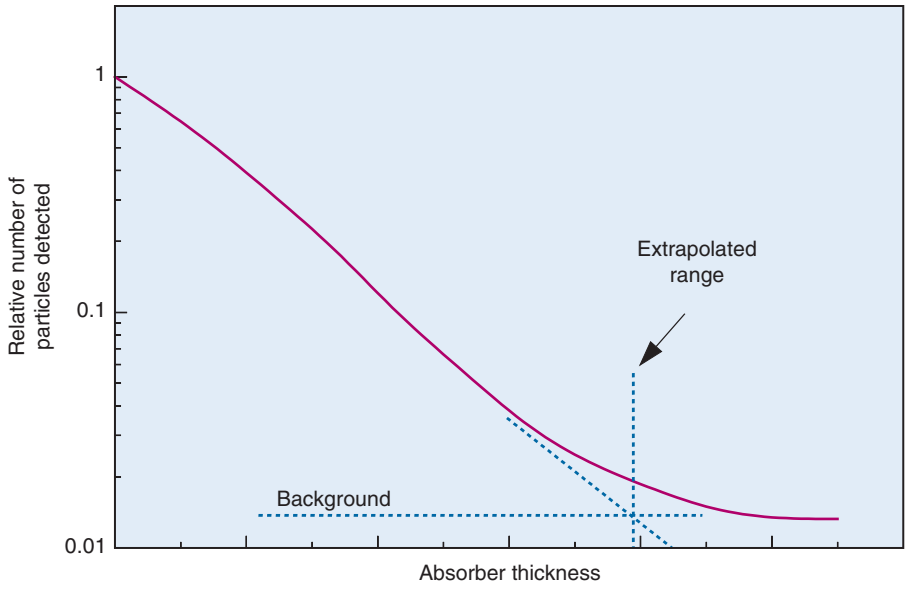

FIGURE 6-9 Relative number of particles detected versus absorber thickness in an electron absorption experiment. Compare with Figure 6-8.

the curve is called the *extrapolated range* R_e of the electrons. This is slightly less (perhaps by a few percent) than the maximum range R_m, which is the actual maximum thickness of absorber penetrated by the maximum energy β particles (Fig. 6-9); however, because the difference is small and because R_m is very difficult to measure, R_e usually is specified as the maximum β-particle range.

The extrapolated range for a monoenergetic beam of electrons of energy E is the same as that for a beam of β particles of maximum energy $E_\beta^{max} = E$. In both cases, range is determined by the maximum energy of electrons in the beam. The shapes of the transmission curves for monoenergetic electrons and for β particles are somewhat different, however. Specifically, the curve for β particles declines more rapidly for very thin absorbers because of rapid elimination of low-energy electrons in the β-particle energy spectrum (See Fig. 3-2).

Extrapolated ranges are found to be inversely proportional to the density ρ of the absorbing material. To normalize for density effects, electron ranges usually are expressed in g/cm^2 of absorber. This is the weight of a 1-cm^2 section cut from a thickness of an absorber equal to the range of electrons in it. The range in cm and in g/cm^2 are related according to

$$R_e(\text{g/cm}^2) = R_e(\text{cm}) \times \rho(\text{g/cm}^3)$$
$$R_e(\text{cm}) = R_e(\text{g/cm}^2)/\rho(\text{g/cm}^3) \qquad (6\text{-}8)$$

It also is found that extrapolated ranges in different elements, when expressed in g/cm^2, are practically identical. There are small differences in electron energy loss rates in different elements, as discussed in Section A.4, but they have only a small effect on total ranges.

Figure 6-10 shows a curve for the extrapolated range of electrons in water, in centimeters, versus electron energy (or maximum β-particle energy, E_β^{max}). Because the density of water is 1, this curve is numerically equal to the extrapolated range in g/cm^2 of water, which has the same value for all absorbers. It can be used to determine extrapolated ranges for other absorbers by dividing by the absorber density, as indicated in Equation 6-8.

EXAMPLE 6-5

Using Figure 6-10, determine the range of 1-MeV electrons in air (ρ = 0.001293 g/cm^3) and lead (ρ = 11.3 g/cm^3).

Answer

From Figure 6-10, the range of a 1-MeV electron in water (ρ = 1 g/cm^3) is 0.4 cm, or 0.4 g/cm^2. Thus

$$R_e \text{ (air)} = (0.4 \text{ g/cm}^2)/0.001293 \text{ g/cm}^3$$
$$\approx 309 \text{ cm}$$
$$R_e \text{ (lead)} = (0.4 \text{ g/cm}^2)/11.3 \text{ g/cm}^3$$
$$\approx 0.035 \text{ cm}$$

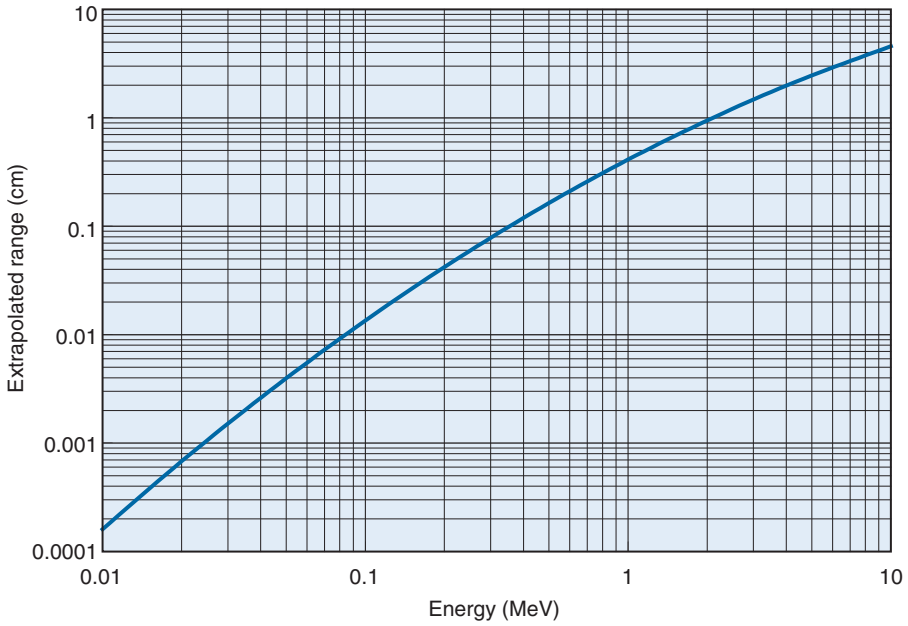

FIGURE 6-10 Extrapolated range in water versus electron energy. The curve is derived from Equation 3-3 in Chapter 21 of reference 1. Curve applies to other absorbers by dividing range in water by absorber density, ρ, in g/cm^3.

Example 6-5 illustrates that extrapolated ranges can be several meters in air but that they are only a few millimeters or fractions of a millimeter in solid materials or liquids. Some ranges for β particles emitted by radionuclides of medical interest are summarized in Table 6-1.

The *average range* for electrons is the thickness required to stop 50% of an electron beam. From Figure 6-9, it is evident that this is much smaller than the extrapolated range. It is found experimentally that the average range for a β-particle beam is given by[1]

$$\bar{D}_{1/2}(\text{cm}) \approx 0.108 \times [E_\beta^{\max}]^{1.14}/\rho(\text{g/cm}^3) \qquad (6\text{-}9)$$

where $E_\beta^{\max}$ is the maximum energy of the β particles in MeV and ρ is the density of the absorbing material. The average range of positrons plays a significant role in imaging with positron-emitting radionuclides, where it places a fundamental limit on obtainable

TABLE 6-1
BETA-PARTICLE RANGES FOR SOME COMMONLY USED β$^+$ AND β$^-$ EMITTERS*

		Extrapolated Range (cm) in			Average Range (cm) in
Radionuclide	**E_β^{max} (MeV)**	**Air**	**Water**	**Aluminum**	**Water**
^{3}H	0.0186	4.5	0.00059	0.00022	—
^{11}C	0.961	302	0.39	0.145	0.103
^{14}C†	0.156	21.9	0.028	0.011	0.013
^{13}N	1.19	395	0.51	0.189	0.132
^{15}O	1.723	617	0.80	0.295	0.201
^{18}F	0.635	176	0.23	0.084	0.064
^{32}P	1.70	607	0.785	0.290	0.198
^{82}Rb	3.35	1280	1.65	0.612	0.429

*Extrapolated and average ranges calculated from Equations 3-3 and 3-7, respectively, in Chapter 21 of reference 1.
†Ranges for ^{35}S ($E_\beta^{\max}$ = 0.167 MeV) are nearly the same as those for ^{14}C.

spatial resolution. This is discussed in Chapter 18, Section A.4. Average ranges in water ($\rho = 1$) also are listed in Table 6-1. Average ranges in soft tissue are essentially the same as for water.

C. PASSAGE OF HIGH-ENERGY PHOTONS THROUGH MATTER

1. Photon Interaction Mechanisms

High-energy photons (γ rays, x rays, annihilation radiation, and bremsstrahlung) transfer their energy to matter in complex interactions with atoms, nuclei, and electrons. For practical purposes, however, these interactions can be viewed as simple collisions between a photon and a target atom, nucleus, or electron. These interactions do not cause ionization directly, as do the charged-particle interactions; however, some of the photon interactions result in the ejection of orbital electrons from atoms or in the creation of positive-negative electron pairs. These electrons in turn cause ionization effects, which are the basis for mechanisms by which high-energy photons are detected and by which they cause radiobiologic effects. For these reasons, high-energy photons are classified as *secondary ionizing radiation.*

There are nine possible interactions between photons and matter, of which only four are of significance to nuclear medicine. These four interactions, and mathematical aspects of the passage of photon beams through matter, are discussed.

2. The Photoelectric Effect

The *photoelectric effect* is an atomic absorption process in which an atom absorbs totally the energy of an incident photon. The photon disappears and the energy absorbed is used to eject an orbital electron from the atom. The ejected electron is called a *photoelectron.* It receives kinetic energy E_{pe}, equal to the difference between the incident photon energy E_0 and the binding energy of the electron shell from which it was ejected. For example, if a K-shell electron is ejected, the kinetic energy of the photoelectron is

$$E_{pe} = E_0 - K_B \qquad (6\text{-}10)$$

where K_B is the K-shell binding energy for the atom from which it is ejected (see Chapter 2, Section C.2). The photoelectric effect looks like a "collision" between a photon and an orbital electron in which the electron is ejected from the atom and the photon disappears (Fig. 6-11).

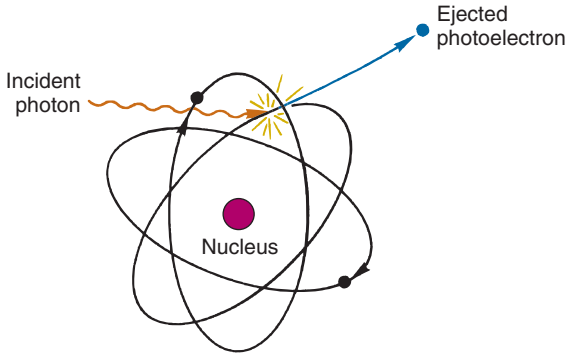

FIGURE 6-11 Schematic representation of the photoelectric effect. The incident photon transfers its energy to a photoelectron and disappears.

Photoelectrons cannot be ejected from an electron shell unless the incident photon energy exceeds the binding energy of that shell. (Values of K-shell binding energies for the elements are listed in Appendix B.) If sufficient photon energy is available, the photoelectron is most likely to be ejected from the innermost possible shell. For example, ejection of a K-shell electron is four to seven times more likely than ejection of an L-shell electron when the energy requirement of the K shell is met, depending on the absorber element.

The photoelectric effect creates a vacancy in an orbital electron shell, which in turn leads to the emission of characteristic x rays (or Auger electrons). In low-Z elements, binding energies and characteristic x-ray energies are only a few keV or less. Thus binding energy is a small factor in photoelectric interactions in body tissues. In heavier elements, however, such as iodine or lead, binding energies are in the 20- to 100-keV range, and they may account for a significant fraction of the absorbed photon energy.

The kinetic energy imparted to the photoelectron is deposited near the site of the photoelectric interaction by the ionization and excitation interactions of high-energy electrons described in Section A. Extrapolated ranges for photoelectrons of various energies in soft tissue can be determined from Figure 6-10.

3. Compton Scattering

Compton scattering is a "collision" between a photon and a loosely bound outer-shell orbital electron of an atom. In Compton scattering, because the incident photon energy greatly exceeds the binding energy of the electron to

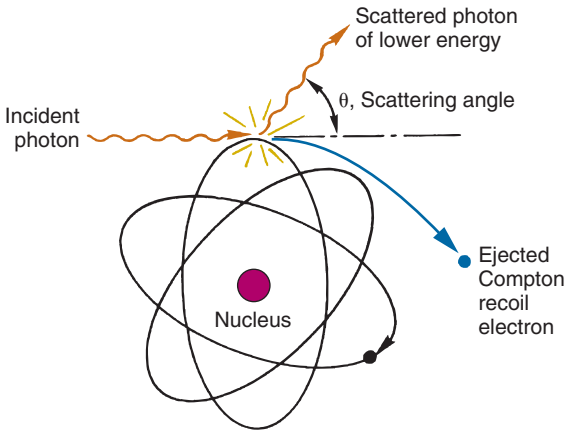

FIGURE 6-12 Schematic representation of Compton scattering. The incident photon transfers part of its energy to a Compton recoil electron and is scattered in another direction of travel (θ, scattering angle).

the atom, the interaction looks like a collision between the photon and a "free" electron (Fig. 6-12).

The photon does not disappear in Compton scattering. Instead, it is deflected through a scattering angle θ. Part of its energy is transferred to the *recoil electron*; thus the photon loses energy in the process. The energy of the scattered photon is related to the scattering angle θ by considerations of energy and momentum conservation according to*

$$E_{sc} = E_0/[1 + (E_0/0.511)\,(1 - \cos\theta)] \quad (6\text{-}11)$$

where E_0 and E_{sc} are the incident and scattered photon energies in MeV, respectively. The energy of the recoil electron, E_{re}, is thus

$$E_{re} = E_0 - E_{sc} \quad (6\text{-}12)$$

*Derivations of Compton energy-angle relationships can be found in Chapter 23 of reference 1.

The energy transferred does not depend on the density, atomic number, or any other property of the absorbing material. Compton scattering is strictly a photon-electron interaction.

The amount of energy transferred to the recoil electron in Compton scattering ranges from nearly zero for θ ≈ 0 degrees ("grazing" collisions) up to a maximum value E_{re}^{max} that occurs in 180-degree *backscattering events.* The minimum energy for scattered photons, E_{sc}^{min}, also occurs for 180-degree backscattering events. The minimum energy of Compton-scattered photons can be calculated from Equation 6-11 with θ = 180 degrees (cos 180° = –1):

$$E_{sc}^{min} = E_0/[1 + (2E_0/0.511)] \quad (6\text{-}13)$$

Thus

$$\begin{aligned} E_{re}^{max} &= E_0 - E_{sc}^{min} \\ &= E_0\left[1 - \frac{1}{[1 + (2E_0/0.511)]}\right] \\ &= E_0^2/(E_0 + 0.2555) \end{aligned} \quad (6\text{-}14)$$

The minimum energy of backscattered photons, E_{sc}^{min}, and the maximum energy transferred to the recoil electron, E_{re}^{max}, have characteristic values that depend on E_0, the energy of the incident photon. These energies are of interest in pulse-height spectrometry because they result in characteristic structures in pulse-height spectra (see Chapter 10, Section B.1).

Table 6-2 lists some values of E_{sc}^{min} and E_{re}^{max} for some γ-ray and x-ray emissions from radionuclides of interest in nuclear medicine. Note that for relatively low photon energies (e.g., ^{125}I, 27.5 keV), the recoil electron receives only a small fraction of the incident

TABLE 6-2
SCATTERED PHOTON AND RECOIL ELECTRON ENERGIES FOR 180-DEGREE COMPTON SCATTERING INTERACTIONS

Radionuclide	Photon Energy (keV)	E_{sc}^{min} (keV)	E_{re}^{max} (keV)
^{125}I	27.5	24.8	2.7
^{133}Xe	81	62	19
^{99m}Tc	140	91	49
^{131}I	364	150	214
β^+ (annihilation)	511	170	341
^{60}Co	1330	214	1116
—	∞	255.5	—

photon energy, even in 180-degree scattering events. Thus photon energy changes very little in Compton scattering at low photon energies. The smallness of this energy change has important implications for the elimination of Compton-scattered photons by energy-discrimination techniques (See Fig. 10-10). At higher energies the energy distribution changes and E_{sc}^{min} approaches a maximum value of 255.5 keV. The remaining energy, which now accounts for most of the incident photon energy, is transferred to the recoil electron in 180-degree scattering events. Note also that the energy of Compton-scattered photons never is zero—that is, a photon cannot transfer all its energy to an electron in a Compton scattering event.

The angular distribution of Compton-scattered photons also depends on the incident photon energy. Figure 6-13 shows the relative probability of scattering at different angles per unit of solid angle. Solid angle is proportional to the area subtended on a sphere divided by the total area of the sphere (see also Fig. 11-1). Thus Figure 6-13 reflects the relative number of scattered photons that would be recorded by a detector of fixed area as it was moved about at a fixed distance from the scattering object at different angles relative to the incident beam (in the absence of attenuation, secondary scattering, etc). At relatively low energies (10-100 keV) the highest intensity of Compton-scattered photons would be detected in either the forward or backward direction, with a minimum at right angles (90 degrees) to the direction of the incident photons. At higher energies ($\gg$0.5 MeV), the highest intensity detected would be increasingly toward the forward direction (scattering angle ~0°).

4. Pair Production

Pair production occurs when a photon interacts with the electric field of a charged particle. Usually the interaction is with an atomic nucleus, but occasionally it is with an electron. In pair production, the photon disappears and its energy is used to create a positron-electron pair (Fig. 6-14). Because the positron and electron both have a rest mass equivalent to 0.511 MeV, a minimum photon energy of 2 × 0.511 MeV = 1.022 MeV must be available for pair production to occur. The difference between the incident photon energy E_0 and the 1.022 MeV of energy required to create the electron pair is imparted as kinetic energy to the positron (E_{e^+}) and the electron, (E_{e^-})

$$E_{e^+} + E_{e^-} = E_0 - 1.022\ \text{MeV} \qquad (6\text{-}15)$$

The energy sharing between the electron and positron is more or less random from one interaction to the next, usually within the 20% to 80% sharing range.

The electron and positron dissipate their kinetic energy primarily in ionization and excitation interactions. When the positron

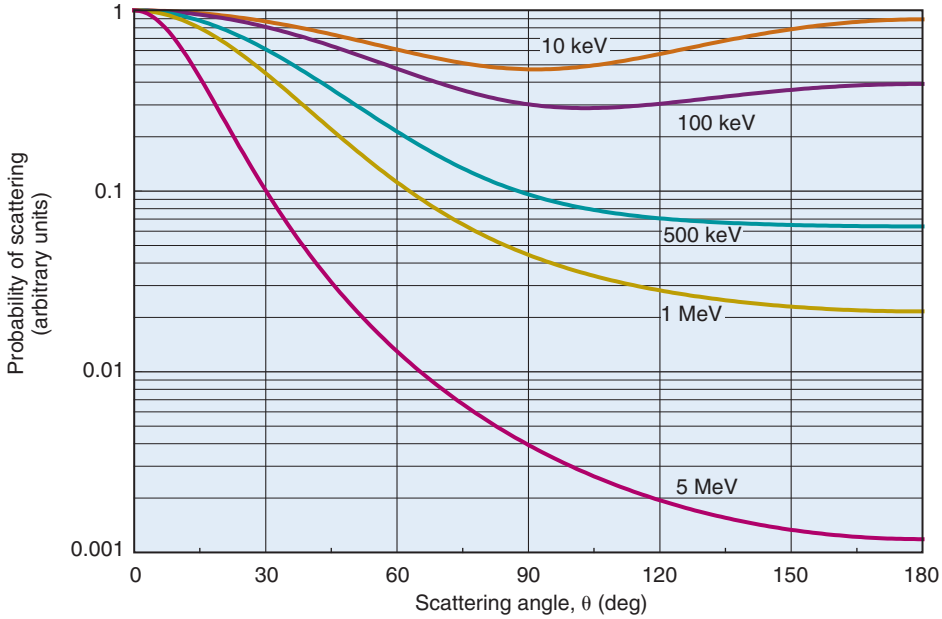

FIGURE 6-13 Relative probability of Compton scattering (arbitrary units) per unit of solid angle versus scattering angle θ for different incident photon energies.

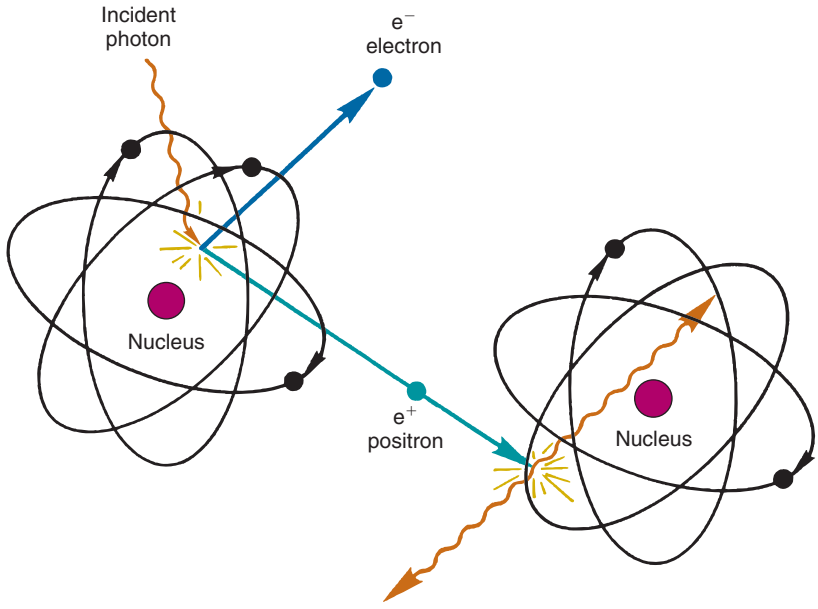

FIGURE 6-14 Schematic representation of pair production. Energy of incident photon is converted into an electron and a positron (total 1.022-MeV mass-energy equivalent) plus their kinetic energy. The positron eventually undergoes mutual annihilation with a different electron, producing two 0.511-MeV annihilation photons.

has lost its kinetic energy and stopped, it undergoes mutual annihilation with a nearby electron, and a pair of 0.511-MeV *annihilation photons* are emitted in opposite directions from the site of the annihilation event (see Chapter 3, Section G). Annihilation photons usually travel for some distance before interacting again. Thus usually only the kinetic energy of the electron and positron (Equation 6-15) is deposited at the site of the pair production event.

5. Coherent (Rayleigh) Scattering

Coherent or *Rayleigh scattering* is a type of scattering interaction that occurs between a photon and an atom as a whole. Because of the great mass of an atom (e.g., in comparison to the recoil electron in the Compton scattering process), very little recoil energy is absorbed by the atom. The photon is therefore deflected with essentially no loss of energy.

Coherent scattering is important only at relatively low energies ($\ll$50 keV). It can be of significance in some precise photon transmission measurements—for example, in x-ray computed tomographic scanning—because it is a mechanism by which photons are removed from a photon beam. Coherent scattering also is an important interaction in x-ray crystallography; however, because it is not an effective mechanism for transferring photon energy to matter, it is of little practical importance in nuclear medicine.

6. Deposition of Photon Energy in Matter

The most important interactions in the transfer of photon energy to matter are the photoelectric effect, Compton scattering, and pair production. The transfer of energy occurs typically in a series of these interactions in which energy is transferred to electrons, and, usually, secondary photons, of progressively less energy (Fig. 6-15). The products of each interaction are secondary photons and high-energy electrons (Table 6-3). The high-energy

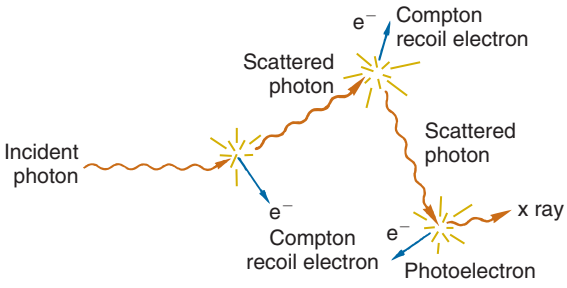

FIGURE 6-15 Multiple interactions of a photon passing through matter. Energy is transferred to electrons in a sequence of photon-energy degrading interactions.

electrons ultimately are responsible for the deposition of energy in matter. Ionization and excitation by these electrons are the mechanisms underlying all of the photon detectors described in Chapter 7. The electrons also are responsible for radiobiologic effects caused by γ-ray, x-ray, or bremsstrahlung radiation. Because of this, the average linear energy transfer of photons for radiobiologic purposes is the same as for electrons of similar energy, that is, 0.2-2 keV/μm (see Chapter 23).

TABLE 6-3
PRODUCTS OF THE THREE MAJOR PHOTON INTERACTION PROCESSES

Interaction	Secondary Photon(s)	High-Energy Secondary Electron(s)
Photoelectric	Characteristic x rays	Photoelectrons
		Auger electrons
Compton	Scattered photon	Recoil electron
Pair production	Annihilation photons	Positive-negative electron pair

D. ATTENUATION OF PHOTON BEAMS

1. Attenuation Coefficients

When a photon passes through a thickness of absorber material, the probability that it will experience an interaction depends on its energy and on the composition and thickness of the absorber. The dependence on thickness is relatively simple; the thicker the absorber, the greater the probability that an interaction will occur. The dependence on absorber composition and photon energy, however, is more complicated.

Consider the photon transmission measurement diagrammed in Figure 6-16. A beam of photons of intensity I (photons/cm^2 • sec) is directed onto an absorber of thickness Δx. Because of composition and photon energy effects, it will be assumed for the moment that the absorber is composed of a single element of atomic number Z and that the beam is monoenergetic with energy E. A photon detector records transmitted beam intensity. It is assumed that only those photons passing through the absorber without interaction are recorded. (The validity of this assumption is discussed further in Sections D.2 and D.3.)

For a "thin" absorber, such that beam intensity is reduced by only a small amount ($\lesssim$10%), it is found that the fractional decrease in beam intensity ($\Delta I/I$) is related to absorber thickness Δx according to

$$\Delta I/I \approx -\mu_l \times \Delta x \qquad (6\text{-}16)$$

the minus sign indicating beam intensity decreases with increasing absorber thickness. The quantity μ_l is called the *linear attenuation coefficient* of the absorber. It has dimensions (thickness)$^{-1}$ and usually is expressed in cm^{-1}. This quantity reflects the "absorptivity" of the absorbing material.

The quantity μ_l is found to increase linearly with absorber density ρ. Density effects are factored out by dividing μ_l by density ρ:

$$\mu_m = \mu_l/\rho \qquad (6\text{-}17)$$

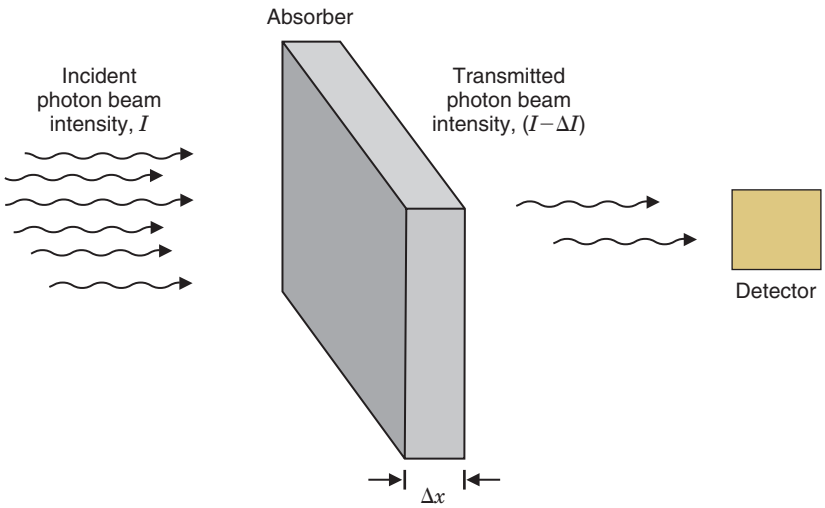

FIGURE 6-16 Photon-beam transmission measurement.

The quantity μ_m has dimensions of cm^2/g and is called the *mass attenuation coefficient* of the absorber. It depends on the absorber atomic number Z and photon energy E. This sometimes is emphasized by writing it as $\mu_m(Z, E)$.

It is possible to measure μ_m or μ_l in different absorber materials by transmission measurements with monoenergetic photon beams. Most tables, however, are based on theoretical calculations from atomic and nuclear physics. An extensive tabulation of values of μ_m versus photon energy for different absorber materials is found in reference 2. Some values of interest to nuclear medicine, taken from these tables, are presented in Appendix D. Usually, values of μ_m rather than μ_l are tabulated because μ_m does not depend on the physical state (density) of the absorber. Given a value of μ_m from the tables, μ_l for an absorber can be obtained from

$$\mu_l(\text{cm}^{-1}) = \mu_m(\text{cm}^2/\text{g}) \times \rho(\text{g/cm}^3) \quad (6\text{-}18)$$

The mass attenuation coefficient for a *mixture of elements* can be obtained from the values for its component elements according to

$$\mu_m(\text{mix}) = \mu_{m,1} f_1 + \mu_{m,2} f_2 + \cdots \quad (6\text{-}19)$$

where $\mu_{m,1}$, $\mu_{m,2}$ … are the mass attenuation coefficients for elements 1, 2, …, and f_1, f_2, …, are the fractions by weight of these elements in the mixture. For example, the mass attenuation coefficient for water (2/18 H, 16/18 O, by weight) is given by

$$\mu_m(\text{water}) = (2/18)\mu_m(\text{H}) + (16/18)\mu_m(\text{O}) \quad (6\text{-}20)$$

The mass attenuation coefficient μ_m can be broken down into components according to

$$\mu_m = \tau + \sigma + \kappa \quad (6\text{-}21)$$

where τ is that part of μ_m caused by the photoelectric effect, σ is the part caused by Compton scattering, and κ is the part caused by pair production. Thus, for example, τ would be the mass attenuation coefficient of an absorber in the absence of Compton scattering and pair production. Note that μ_m involves both absorption and scattering processes. Thus μ_m is properly called an *attenuation coefficient* rather than an *absorption coefficient*.

The relative magnitudes of τ, σ, and κ vary with atomic number Z and photon energy E. Figure 6-17 shows graphs of μ_m and its components, τ, σ, and κ versus photon energy from 0.01-10 MeV in water, NaI(Tl), and lead. The following points are illustrated by these graphs:

1. The photoelectric component τ decreases rapidly with increasing photon energy and increases rapidly with increasing atomic number of the absorber ($\tau \propto Z^3/E^3$). The photoelectric effect is thus the dominating effect in heavy elements at low photon energies. The photoelectric component also increases abruptly at energies corresponding to orbital electron binding energies of the absorber elements. At the K-shell binding energies of iodine (K_B = 33.2 keV) and lead (K_B = 88.0 keV), the increase is a factor of 5-6. These abrupt increases are called *K absorption edges*. They result from the fact that photoelectric absorption involving K-shell electrons cannot occur until the photon energy exceeds the K-shell binding energy. L absorption edges also are seen at $E \sim$ 13-16 keV in the graph for lead. L absorption edges in water and iodine and the K absorption edge for water also exist, but they occur at energies less than those shown in the graphs.
2. The Compton-scatter component σ decreases slowly with increasing photon energy E and with increasing absorber atomic number Z. The changes are so small that for practical purposes σ usually is considered to be invariant with Z and E. Compton scattering is the dominating interaction for intermediate values of Z and E.
3. The pair-production component κ is zero for photon energies less than the threshold energy of 1.02 MeV for this interaction; then it increases logarithmically with increasing photon energy and with increasing atomic number of the absorber ($\kappa \propto Z \log E$). Pair production is the dominating effect at higher photon energies in absorbers of high atomic number.

Figure 6-18 shows the dominating (most probable) interaction versus photon energy E and absorber atomic number Z. Note that Compton scattering is the dominating interaction for $Z \lesssim 20$ (body tissues) over most of the nuclear medicine energy range.

2. Thick Absorbers, Narrow-Beam Geometry

The transmission of a photon beam through a "thick" absorber—that is, one in which the probability of photon interaction is not "small" (≥10%)—depends on the geometric

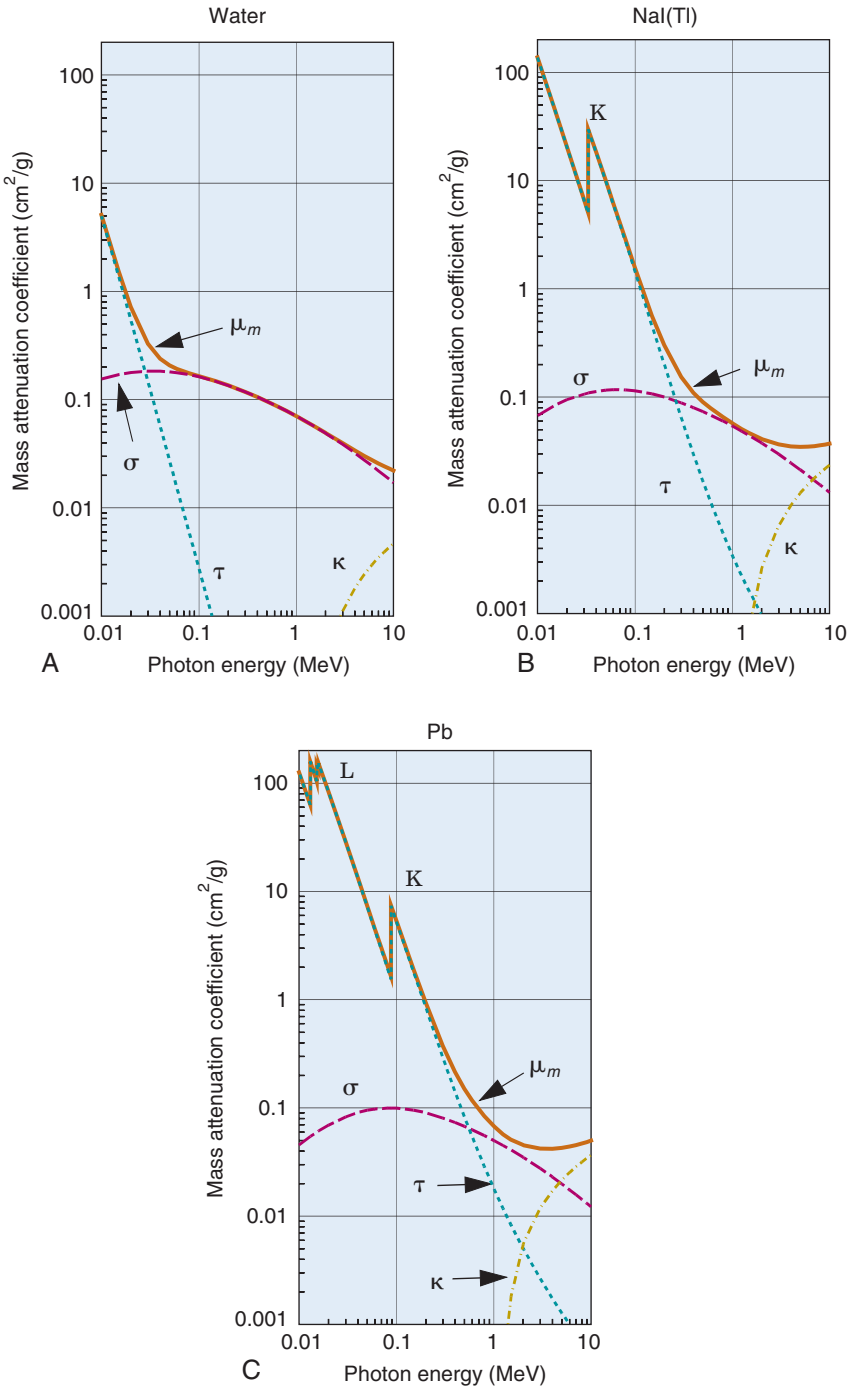

FIGURE 6-17 Photoelectric (τ), Compton (σ), pair-production (κ), and total (μ_m) mass attenuation coefficients (square centimeters per gram) for water (*A*), NaI(Tl) (*B*), and Pb (*C*) from 0.01 to 10 MeV. K and L are absorption edges. Data taken from reference 2. Curves for μ_l can be obtained by multiplying by the appropriate density values.

arrangement of the photon source, absorber, and detector. Specifically, transmission depends on whether scattered photons are recorded as part of the transmitted beam. An arrangement that is designed to minimize the recording of scattered photons is called *narrow-beam geometry*. Conversely, an arrangement in which many scattered photons are recorded is called *broad-beam geometry*. (They also are called *good geometry* and *poor geometry*, respectively.) Figure 6-19 shows examples of these geometries.

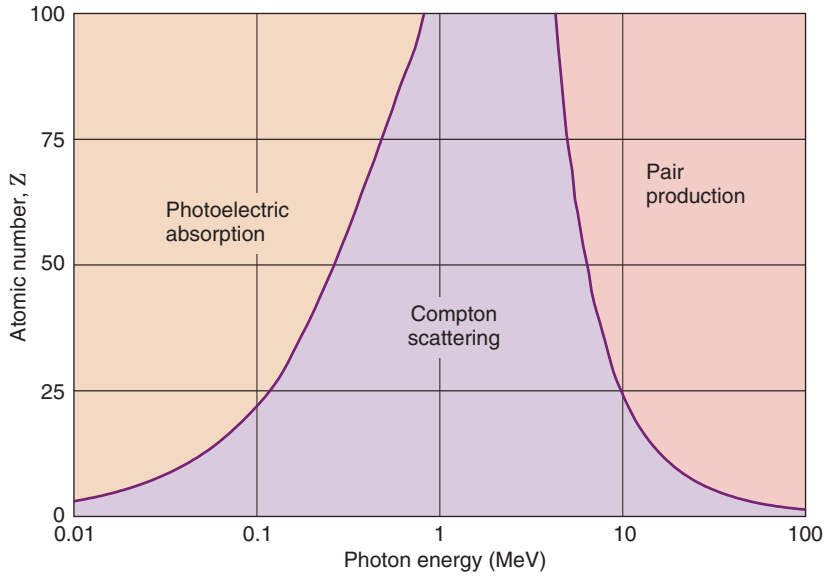

FIGURE 6-18 Predominating (most probable) interaction versus photon energy for absorbers of different atomic numbers. Curves were generated using values obtained from reference 2.

Conditions of narrow-beam geometry usually require that the beam be collimated with a narrow aperture at the source so that only a narrow beam of photons is directed onto the absorber. This minimizes the probability that photons will strike neighboring objects (e.g., the walls of the room or other parts of the measurement apparatus) and scatter toward the detector. Matching collimation on the detector helps prevent photons that are multiple-scattered in the absorber from being recorded. In addition, it is desirable to place the absorber approximately halfway between the source and the detector.

Under conditions of narrow-beam geometry, the transmission of a monoenergetic photon beam through an absorber is described by an exponential equation

$$I(x) = I(0)\, e^{-\mu_l x} \tag{6-22}$$

where $I(x)$ is the beam intensity transmitted through a thickness x of absorber, $I(0)$ is the intensity recorded with no absorber present, and μ_l is the linear attenuation coefficient of the absorber at the photon energy of interest. In contrast to charged particles, photons do not have a definite maximum range. There is always some finite probability that a

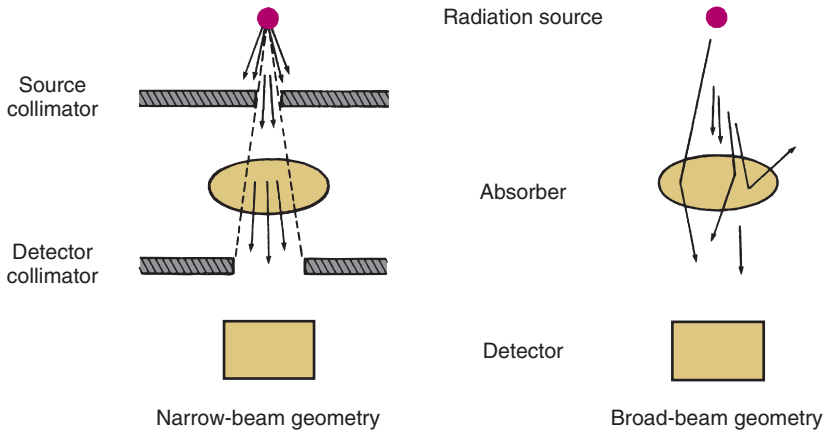

FIGURE 6-19 Narrow-beam and broad-beam geometries for photon-beam attenuation measurements. Narrow-beam geometry is designed to minimize the number of scattered photons recorded.

photon will penetrate even the thickest absorber [i.e., $I(x)$ in Equation 6-22 never reaches zero].

Equation 6-22 is exactly analogous to Equation 4-6 for the decay of radioactivity, with the attenuation coefficient μ_l replacing the decay constant λ and absorber thickness x replacing decay time t. Analogous to the concept of half-life in radioactive decay, the thickness of an absorber that decreases recorded beam intensity by one half is called the *half-value thickness* (HVT) or *half-value layer* (HVL). It is related to the linear attenuation coefficient according to

$$\begin{aligned} \text{HVT} &= \ln 2/\mu_l \\ \mu_l &= \ln 2/\text{HVT} \end{aligned} \qquad (6\text{-}23)$$

where $\ln 2 \approx 0.693$. Compare these equations with Equations 4-8 and 4-9.

Some radiation-shielding problems require the use of relatively thick absorbers; for this purpose it is sometimes useful to know the *tenth-value thickness* (TVT)—that is, the thickness of absorber that decreases transmitted beam intensity by a factor of 10. This quantity is given by

$$\begin{aligned} \text{TVT} &= \ln 10/\mu_l \\ &\approx 3.32 \times \text{HVT} \end{aligned} \qquad (6\text{-}24)$$

where $\ln 10 \approx 2.30$. Some HVTs for water and TVTs for lead are listed in Table 6-4.

The quantity

$$X_m = 1/\mu_l \qquad (6\text{-}25)$$

is called the *mean free path* for photons in an absorber. It is the *average distance* traveled by a photon in the absorber before experiencing an interaction. Mean free path is related to HVT according to

$$\begin{aligned} X_m &= \text{HVT}/\ln 2 \\ &\approx 1.44 \times \text{HVT} \end{aligned} \qquad (6\text{-}26)$$

Note the analogy to average lifetime, τ (Equation 4-12).

Table 6-5 compares mean free paths for photons in water against maximum ranges for electrons in water and α particles in air as

TABLE 6-4

HALF-VALUE THICKNESSES IN WATER AND TENTH-VALUE THICKNESSES IN LEAD (NARROW-BEAM CONDITIONS)

Radionuclide	Photon Energy (keV)	HVT in Water (cm)	TVT in Lead (mm)
^{125}I	27.5	1.7	0.06
^{133}Xe	81	4.3	1.0
^{99m}Tc	140	4.6	0.9
^{131}I	364	6.3	7.7
β^+ (annihilation)	511	7.1	13.5
^{60}Co	1330	11.2	36.2

HVT, half-value thickness; TVT, tenth-value thickness.

TABLE 6-5

COMPARISON OF PHOTON MEAN FREE PATHS AND MAXIMUM ELECTRON AND α-PARTICLE RANGES

Photon or Particle Energy (MeV)	Photon MFP (cm H_2O)	Electron Range (cm H_2O)	α-Particle Range (cm air)
0.01	0.20	0.00016	—
0.1	5.95	0.014	0.1
1	14.14	0.41	0.5
10	45.05	4.6	10.3

MFP, mean free path.

a function of their energy. Although the concepts of photon mean free path and charged particle ranges are different, the comparison gives an indication of relative penetration of photons versus particle radiation. Over the energy range 0.01-10 MeV, photons are much more penetrating than electrons or α particles. For this reason they sometimes are called *penetrating* radiation.

The quantity $e^{-\mu_l x}$ [or $I(x)]/I(0)$ in Equation 6-22], the fraction of beam intensity transmitted by an absorber, is called its *transmission factor*. The transmission factor can be determined using the methods described for determining decay factors in Chapter 4, Section C. For example, the graph shown in Figure 4-3 can be used with "decay factor" replaced by "transmission factor" and "number of half-lives" replaced by "number of HVTs."

EXAMPLE 6-6

Determine the transmission factor for 140-keV photons in 10 cm of soft tissue (water) by direct calculation.

Answer

From Table 6-4, HVT = 4.6 cm in water at 140 keV. Thus $\mu_l = 0.693/4.6 = 0.151$ cm^{-1}, and the transmission factor is

$$I(10)/I(0) = e^{-0.151\times 10} = e^{-1.51}$$

Using a pocket calculator

$$e^{-1.51} = 0.221$$

Thus the transmission factor for 140-keV photons through 10 cm of water is 22.1%.

EXAMPLE 6-7

Estimate the transmission factor for 511-keV photons in 1 cm of lead using graphical methods (see Fig. 4-3).

Answer

From Table 6-4, the TVT of 511-keV photons in lead is 13.5 mm. From Equation 6-24, HVT ≈ TVT/3.32 so for 511-keV photons in lead, HVT = 1.35 cm/3.32 = 0.4 cm. Thus 1 cm = 2.5 HVTs. From Figure 4-3, the transmission (decay) factor for 2.5 HVTs ($T_{1/2}$) is approximately 0.18 (18% transmission).

It must be remembered that the answers obtained in Examples 6-6 and 6-7 apply only to narrow-beam conditions. Broad-beam conditions are discussed in the following section.

3. Thick Absorbers, Broad-Beam Geometry

Practical problems of photon-beam attenuation in nuclear medicine usually involve broad-beam conditions. Examples are the shielding of radioactive materials in lead containers and the penetration of body tissues by photons emitted from radioactive tracers localized in internal organs. In both of these examples, a considerable amount of scattering occurs in the absorber material surrounding or overlying the radiation source.

The factor by which transmission is increased in broad-beam conditions, relative to narrow-beam conditions, is called the *buildup factor B*. Thus the transmission factor T for broad-beam conditions is given by

$$T = Be^{-\mu_l x} \qquad (6\text{-}27)$$

where μ_l and x are the linear attenuation coefficient and thickness, respectively, of the absorber.

Buildup factors for various source-absorber-detector geometries have been calculated. Some values for water and lead for a source embedded in or surrounded by scattering and absorbing material are listed in Table 6-6. Note that B depends on photon energy and on the product $\mu_l x$ for the absorber.

EXAMPLE 6-8

In Example 6-7, the transmission factor for 511-keV photons in 1 cm of lead was found to be 18% for narrow-beam conditions. Estimate the actual transmission for broad-beam conditions (e.g., a vial of β^+-emitting radioactive solution in a lead container of 1-cm wall thickness).

Answer

For 511-keV photons, HVT = 0.4 cm (Example 6-7). Thus $\mu_l = 0.693/(0.4\text{ cm}) \approx 1.73$ cm^{-1}, and, for $x = 1$ cm, $\mu_l x \approx 1.73$. Taking values for 0.5 MeV (≈ 511 keV) from Table 6-6 and using linear interpolation between values for $\mu_l x = 1$ ($B = 1.24$) and $\mu_l x = 2$ ($B = 1.39$), one obtains

$$B = 1.24 + (0.73)(1.39 - 1.24)$$
$$= 1.35$$

For $B = 1.35$, the transmission in broad-beam conditions is 35% greater than calculated for narrow-beam conditions. Thus the actual transmission factor is

$$T \approx 1.35 \times 0.18$$
$$\approx 0.24$$

or 24%.

TABLE 6-6
EXPOSURE BUILDUP FACTORS IN WATER AND IN LEAD*

Material	Photon Energy (MeV)	μx						
		1	*2*	*4*	*7*	*10*	*15*	*20*
Water	0.1	4.55	11.8	41.3	137	321	938	2170
	0.5	2.44	4.88	12.8	32.7	62.9	139	252
	1.0	2.08	3.62	7.68	15.8	26.1	47.7	74.0
	2.0	1.83	2.81	4.98	8.65	12.7	20.1	28.0
	4.0	1.63	2.24	3.46	5.30	7.16	10.3	13.4
	6.0	1.51	1.97	2.84	4.12	5.37	7.41	9.42
	10.0	1.37	1.68	2.25	3.07	3.86	5.19	6.38
Lead	0.5	1.24	1.39	1.62	1.88	2.10	2.39	2.64
	1.0	1.38	1.68	2.19	2.89	3.51	4.45	5.27
	2.0	1.40	1.76	2.52	3.74	5.07	7.44	9.08
	4.0	1.36	1.67	2.40	3.79	5.61	9.73	15.4
	6.0	1.42	1.73	2.49	4.13	6.61	13.7	26.6
	10.0	1.51	2.01	3.42	7.37	15.4	50.8	161

*Data taken from Schleien B (ed): *The Health Physics and Radiological Health Handbook*. Silver Spring, MD, 1992, Scinta.[3]

Example 6-8 illustrates that scatter effects can be significant in broad-beam conditions. The thickness of lead shielding required to achieve a given level of protection is greater than that calculated using narrow-beam equations.

EXAMPLE 6-9

Estimate the thickness of lead shielding required to achieve an actual transmission of 18% in the problem described in Example 6-8.

Answer

Because $B = 1.35$, it is necessary to further reduce transmission by approximately $1/1.35 \approx 0.74$ to correct for scattered radiation. According to Figure 4-3, this would require approximately 0.45 HVTs, or approximately 0.18 cm (1 HVT = 0.4 cm). This is only an estimate, because the HVT used applies to narrow-beam conditions. A more exact answer could be obtained by successive approximations.

Broad-beam conditions also arise in problems of internal radiation dosimetry—for example, when it is desired to calculate the radiation dose to an organ delivered by a radioactive concentration in another organ. This issue is discussed further in Chapter 22, Section B.

4. Polyenergetic Sources

Many radionuclides emit photons of more than one energy. The photon transmission curve for such an emitter consists of a sum of exponentials, one component for each of the photon energies emitted. The transmission curve has an appearance similar to the decay curve for a mixed radionuclide sample shown in Figure 4-5. The transmission curve drops steeply at first as the lower-energy ("softer") components of the beam are removed. Then it gradually flattens out, reflecting greater penetration by the higher-energy ("harder") components of the beam. The average energy of photons remaining in the beam increases with increasing absorber thickness. This effect is called *beam hardening*.

It is possible to detect small amounts of a high-energy photon emitter in the presence of large amounts of a low-energy photon emitter by making use of the beam-hardening effect. For example, a 3-mm thickness of lead is several TVTs for the 140-keV γ rays of ^{99m}Tc, but it is only approximately 1 HVT for the 700- to 800-keV γ rays of ^{99}Mo. Thus a

3-mm-thick lead shield placed around a vial containing ^{99m}Tc solution permits detection of small amounts of ^{99}Mo contamination with minimal interference from the ^{99m}Tc γ rays. (See Chapter 5, Section C).

REFERENCES

1. Evans RD: *The Atomic Nucleus*, New York, 1972, McGraw-Hill, p 628. (Note: This reference contains useful discussions of many details of radiation interactions with matter.)
2. Berger MJ, Hubbell JH: XCOM: Photon Cross-Sections Database, NIST Standard Reference Database 8 (XGAM) Available at: http://www.nist.gov/pml/data/xcom/index.cfm. (Accessed August 17, 2011.).
3. Schleien B, editor: *The Health Physics and Radiological Health Handbook*, Silver Spring, MD, 1992, Scinta, pp 176-177. (Note: This reference also contains useful tabulations of charged-particle ranges and other absorption data.)

BIBLIOGRAPHY

Discussions of radiation interactions and their passage through matter are found in the following:

Johns HE, Cunningham JR: *The Physics of Radiology*, ed 4, Springfield, IL, 1983, Charles C Thomas, Chapter 6.

Lapp RE, Andrews HL: *Nuclear Radiation Physics*, ed 4, Englewood Cliffs, NJ, 1972, Prentice-Hall, pp 196-203, 233-247, 261-279.

A comprehensive tabulation of x-ray and γ-ray attenuation coefficients can be found in the following reference.

Hubbell JH, Seltzer SM: Tables of X-Ray Mass Attenuation Coefficients and Mass Energy-Absorption Coefficients 1 keV to 20 MeV for Elements Z = 1 to 92 and 48 Additional Substances of Dosimetric Interest. NISTIR 5632, Gaithersburg MD, 1995, US Department of Commerce. Available at: http://physics.nist.gov/PhysRefData/XrayMassCoef/cover.html (Accessed August 26th, 2011.)